World Journal of Gastroenterology

Submit a Manuscript: http://www.wjgnet.com/esps/
Help Desk: http://www.wjgnet.com/esps/helpdesk.aspx
DOI: 10.3748/wjg.v20.i22.6844

World J Gastroenterol 2014 June 14; 20(22): 6844-6859
ISSN 1007-9327 (print) ISSN 2219-2840 (online)
© 2014 Baishideng Publishing Group Inc. All rights reserved.

ORIGINAL ARTICLE

Role of the $Na^+/K^+/2Cl^-$ cotransporter NKCC1 in cell cycle progression in human esophageal squamous cell carcinoma

Atsushi Shiozaki, Yoshito Nako, Daisuke Ichikawa, Hirotaka Konishi, Shuhei Komatsu, Takeshi Kubota, Hitoshi Fujiwara, Kazuma Okamoto, Mitsuo Kishimoto, Yoshinori Marunaka, Eigo Otsuji

Atsushi Shiozaki, Yoshito Nako, Daisuke Ichikawa, Hirotaka Konishi, Shuhei Komatsu, Takeshi Kubota, Hitoshi Fujiwara, Kazuma Okamoto, Eigo Otsuji, Division of Digestive Surgery, Department of Surgery, Kyoto Prefectural University of Medicine, Kyoto 602-8566, Japan
Mitsuo Kishimoto, Department of Pathology, Kyoto Prefectural University of Medicine, Kyoto 602-8566, Japan
Yoshinori Marunaka, Departments of Molecular Cell Physiology and Bio-Ionomics, Graduate School of Medical Science, Kyoto Prefectural University of Medicine, Kyoto 602-8566, Japan
Yoshinori Marunaka, Japan Institute for Food Education and Health, St. Agnes' University, Kyoto 602-8013, Japan
Author contributions: Shiozaki A and Nako Y contributed equally to this work; Shiozaki A and Nako Y designed the study, wrote the manuscript and performed the majority of the experiments; Ichikawa D, Konishi H, Komatsu S, Kubota T, Fujiwara H, Okamoto K and Kishimoto M collected and analyzed the clinicopathological data obtained from ESCC patients; Marunaka Y and Otsuji E were involved in editing the manuscript.
Supported by Grants-in-Aid for Young Scientists (B), NO. 22791295, NO. 23791557, and NO. 24791440; and a Grant-in-Aid for Scientific Research (C), NO.22591464 and NO. 24591957, from the Japan Society for the Promotion of Science
Correspondence to: Atsushi Shiozaki, Assistant Professor, Division of Digestive Surgery, Department of Surgery, Kyoto Prefectural University of Medicine, 465 Kajii-cho, Kamigyo-ku, Kyoto 602-8566, Japan. shiozaki@koto.kpu-m.ac.jp
Telephone: +81-75-2515527 Fax: +81-75-2515522
Received: October 28, 2013 Revised: January 17, 2014
Accepted: February 17, 2014
Published online: June 14, 2014

Abstract

AIM: To investigate the role of $Na^+/K^+/2Cl^-$ cotransporter 1 (NKCC1) in the regulation of genes involved in cell cycle progression and the clinicopathological significance of its expression in esophageal squamous cell carcinoma (ESCC).

METHODS: An immunohistochemical analysis was performed on 68 primary tumor samples obtained from ESCC patients that underwent esophagectomy. NKCC1 expression in human ESCC cell lines was analyzed by Western blotting. Knockdown experiments were conducted using NKCC1 small interfering RNA, and the effects on cell cycle progression were analyzed. The gene expression profiles of cells were analyzed by microarray analysis.

RESULTS: Immunohistochemical staining showed that NKCC1 was primarily found in the cytoplasm of carcinoma cells and that its expression was related to the histological degree of differentiation of SCC. NKCC1 was highly expressed in KYSE170 cells. Depletion of NKCC1 in these cells inhibited cell proliferation *via* G_2/M phase arrest. Microarray analysis identified 2527 genes with altered expression levels in NKCC1depleted KYSE170. Pathway analysis showed that the top-ranked canonical pathway was the G_2/M DNA damage checkpoint regulation pathway, which involves MAD2L1, DTL, BLM, CDC20, BRCA1, and E2F5.

CONCLUSION: These results suggest that the expression of NKCC1 in ESCC may affect the G_2/M checkpoint and may be related to the degree of histological differentiation of SCCs. We have provided a deeper understanding of the role of NKCC1 as a mediator and/or a biomarker in ESCC.

© 2014 Baishideng Publishing Group Inc. All rights reserved.

Key words: $Na^+/K^+/2Cl^-$ cotransporter 1; Esophageal cancer; Cell cycle

Core tip: The objectives of the present study were to investigate the role of $Na^+/K^+/2Cl^-$ cotransporter 1 (NKCC1) in the regulation of genes involved in cell cycle progression and the clinicopathological significance

of its expression in esophageal squamous cell carcinoma (ESCC). An immunohistochemical analysis revealed that the expression of NKCC1 in ESCC samples was related to the histological type. Microarray results suggested that NKCC1 exhibits marked effects on the expression of genes related to G_2/M cell cycle progression. A deeper understanding of the role of NKCC1 may lead to its use as an important biomarker and/or a novel therapeutic target for ESCC treatment.

Shiozaki A, Nako Y, Ichikawa D, Konishi H, Komatsu S, Kubota T, Fujiwara H, Okamoto K, Kishimoto M, Marunaka Y, Otsuji E. Role of the $Na^+/K^+/2Cl^-$ cotransporter NKCC1 in cell cycle progression in human esophageal squamous cell carcinoma. *World J Gastroenterol* 2014; 20(22): 6844-6859 Available from: URL: http://www.wjgnet.com/1007-9327/full/v20/i22/6844.htm DOI: http://dx.doi.org/10.3748/wjg.v20.i22.6844

INTRODUCTION

Several studies have recently shown that ion channels and transporters play important roles in fundamental cellular functions. Their physiological roles in cell proliferation have been studied in more detail because ion transport across the cell membrane is involved in the regulation of cell volume, which is indispensable for cell cycle progression. Several reports have demonstrated the important roles of Cl^- channels/transporters, such as Ca^{2+}- activated $2Cl^-$ channels and Cl^-/HCO^{3-} exchangers, in gastrointestinal cancer cells[1,2]. These studies indicated that transepithelial Cl^- transport plays an important role in the proliferation of gastrointestinal cancer cells.

The $Na^+/K^+/2Cl^-$ cotransporter (NKCC) is a member of the cation-chloride cotransporter family. NKCC transports one sodium ion, one potassium ion, and two chloride ions across the plasma membrane and is sensitive to loop diuretics, such as furosemide and bumetanide. There are two isoforms of NKCC, and NKCC1 is ubiquitously expressed in various types of cells including epithelial cells[3,4]. We previously examined transepithelial Cl^- transport in various types of cancer cells[5-7] and showed that NKCC1 plays an important role in the proliferation of gastric and prostate cancer cells[8,9]. However, the role of NKCC1 in the proliferation of esophageal squamous cell carcinoma (ESCC) cells and its detailed regulatory mechanisms have not been fully investigated. Furthermore, the clinicopathological meaning of NKCC1 expression in ESCCs remains uncertain.

The objectives of the present study were to investigate the role of NKCC1 in the regulation of genes involved in cell cycle progression and the clinicopathological significance of its expression in ESCC. We analyzed the expression of NKCC1 in human ESCC samples and determined its relationship with the degree of histological differentiation of SCC samples. Furthermore, microarray analyses showed that depletion of NKCC1 with small interfering RNA (siRNA) changed the expression levels of many genes involved in G_2/M cell cycle progression. Our results indicate that NKCC1 plays an important role in the tumor progression of ESCCs.

MATERIALS AND METHODS

Cell lines, antibodies, and other reagents

The human ESCC cell lines TE2, TE5, TE9, and TE13 were obtained from the Cell Resource Center for Biomedical Research at the Institute of Development, Aging, and Cancer (Tohoku University, Sendai, Japan)[10]. The human ESCC cell lines KYSE70 and KYSE170 were obtained from Kyoto University (Kyoto, Japan)[11]. These cells were grown in RPMI-1640 medium (Nacalai Tesque, Kyoto, Japan) supplemented with 100 U/mL of penicillin, 100 μg/mL of streptomycin, and 10% fetal bovine serum. Cells were cultured in flasks or dishes in a humidified incubator at 37 ℃ under 5% CO_2 in air.

The anti-NKCC1 antibody used for immunohistochemical analysis and the protein assay were obtained from Sigma-Aldrich (St. Louis, MO). The anti-Ki-67 antibody was purchased from Santa Cruz Biotechnology (Santa Cruz, CA). Horseradish peroxidase (HRP)-conjugated anti-rabbit secondary antibodies were purchased from Cell Signaling Technology (Beverly, MA), and the antibody for glyceraldehyde-3-phosphate dehydrogenase (GAPDH) was obtained from Santa Cruz Biotechnology. Furosemide was purchased from Nacalai Tesque, Inc. (Kyoto, Japan).

Patients and primary tissue samples

ESCC tumor samples were obtained from 68 patients with a histologically confirmed primary ESCC who underwent esophagectomy at Kyoto Prefectural University of Medicine between 1998 and 2007 and were embedded in paraffin after 12 h of formalin fixation. Patient eligibility criteria were as follows: no synchronous or metachronous cancers (in addition to ESCC) and no preoperative chemotherapy or radiation therapy. We excluded patients with non-curative resected tumors or non-consecutive data. All patients provided written informed consent. Relevant clinicopathological and survival data were obtained from the hospital database. Staging was principally based on the International Union Against Cancer/tumor node metastasis Classification of Malignant Tumors (7^{th} edition)[12].

Immunohistochemistry

Paraffin sections (4 μm thick) of tumor tissues were subjected to immunohistochemical staining for the NKCC1 protein using the avidin-biotin-peroxidase method. Briefly, paraffin sections were dewaxed with xylene and dehydrated with a graded series of alcohols. Antigen retrieval was performed by heating the samples in Dako REAL Target Retrieval Solution (Glostrup, Denmark) for 40 min at 98 ℃. Endogenous peroxidases were quenched by incubating the sections for 30 min in 0.3% H_2O_2. Sections were then treated with protein blocker and incu-

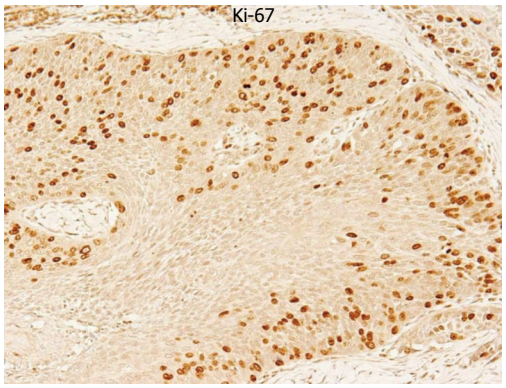

Figure 1 Immunohistochemical staining of a primary tumor sample of human esophageal squamous cell carcinomas with a Ki-67 antibody. The expression of Ki-67 was clearly identified in the nucleus of ESCCs (Magnification × 200).

bated overnight at 4 ℃ with anti-NKCC1 or anti-Ki-67 antibody. The avidin-biotin-peroxidase complex (Vectastain ABC Elite kit; Vector laboratories, Burlingame, CA) was visualized with diaminobenzidine tetrahydrochloride. Sections were counterstained with hematoxylin, dehydrated with a graded series of alcohols, cleared in xylene, and mounted.

Immunohistochemical samples stained with NKCC1 were graded semi-quantitatively by considering both the staining intensity and the percentage of positive tumor cells using an immunoreactive score (IRS)[13]. Staining intensity was scored as 0 (no staining), 1 (weak staining), 2 (moderate staining), or 3 (strong staining). The proportion of positive tumor cells was scored as 1 (1%-10%), 2 (11%-50%), 3 (51%-80%), or 4 (81% or more). Each sample's score was calculated as the maximum multiplied product of the intensity and proportion scores. Scores of 6 or more and scores of less than 6 were defined as high grade and low grade NKCC1 expression, respectively.

Tumor cells with nuclei containing brown immunoreactive products were considered Ki-67 positive (Figure 1). To evaluate the positive staining rate, the number of Ki-67 labeled cells was quantified in five randomly selected fields at a magnification of × 400. The positive staining rate in each case was calculated as the number of positive cells divided by the total number of examined cells in all examined fields. The mean Ki-67 labeling index was 29.4% (range, 2.9%-55.9%) in 68 primary tumor samples.

Western blotting

Cells were harvested in M-PER lysis buffer (Pierce, Rockford, IL) supplemented with protease inhibitors (Pierce, Rockford, IL). The protein concentration was measured with a modified Bradford assay (Bio-Rad, Hercules, CA). Cell lysates containing equal amounts of total protein were separated by SDS-PAGE and then transferred onto PVDF membranes (GE Healthcare, Piscataway, NJ). These membranes were then probed with the indicated antibodies, and proteins were detected using an ECL Plus Western Blotting Detection System (GE Healthcare, Piscataway, NJ).

Small interfering RNA transfection

Cells were transfected with 10 nmol/L NKCC1 Small interfering RNA (siRNA) (Stealth RNAi™ siRNA No.HSS109914; Invitrogen, Carlsbad, CA) using the Lipofectamine RNAiMAX reagent (Invitrogen), according to the manufacturer's instructions. The medium containing siRNA was replaced with fresh medium after 24 h. The control siRNA provided (Stealth RNAi™ siRNA Negative Control; Invitrogen) was used as a negative control.

Cell cycle analysis

The cell cycle phase was evaluated 48 h after siRNA transfection by fluorescence-activated cell scoring (FACS). Briefly, cells were treated with Triton X-100 and RNase, and nuclei were stained with propidium iodide (PI) prior to DNA content measurement using a Becton Dickinson FACS Calibur instrument (Becton Dickinson, Mountain view, CA). At least 10000 cells were analyzed, and ModFit LT software (Verity Software House, Topsham, ME) was used to analyze cell cycle distribution.

Cell proliferation

Cells were seeded in 6-well plates at a density of 1.0×10^5 cells per well and incubated at 37 ℃ with 5% CO_2. siRNA was transfected 24 h after the cells seeded. Cells were detached from the flasks with trypsin-EDTA 72 h after siRNA transfection and were counted using a hemocytometer.

Real time reverse transcription-polymerase chain reaction

Total RNA was extracted using an RNeasy kit (Qiagen, Valencia, CA). Messenger RNA (mRNA) expression was measured by quantitative real-time PCR (7300 Real-Time PCR System; Applied Biosystems, Foster City, CA) with TaqMan Gene Expression Assays (Applied Biosystems), according to the manufacturer's instructions. Expression levels were measured for the following genes: NKCC1 (Hs00169032_m1), MAD2L1 (Hs01554513_g1), DTL (Hs00978565_m1), BLM (Mm00476150_m1), CDC20 (Hs00426680_mH), BRCA1 (Hs01556193_m1), and E2F5 (Hs00231092_m1) (Applied Biosystems). Expression was normalized for each gene to the housekeeping gene beta-actin (ACTB, Hs01060665_g1; Applied Biosystems). Assays were performed in triplicate.

Microarray sample preparation and hybridization

Total RNA was extracted using an RNeasy kit (Qiagen). RNA quality was monitored with an Agilent 2100 Bioanalyzer (Agilent Technologies, Santa Clara, CA). Cyanine-3 (Cy3)-labeled cRNA was prepared from 0.1 μg of total RNA using a Low Input Quick Amp Labeling Kit (Agilent), according to the manufacturer's instructions. Samples were purified using RNeasy columns (Qiagen). A total of 0.60 μg of Cy3-labelled cRNA was

Table 1 Correlations between clinicopathological parameters and $Na^+/K^+/2Cl^-$ cotransporter 1 expression

Variable		NKCC1 expression		*P* value
		Low grade	High grade	
Age (yr)	< 60	12	10	0.1874
	⩾ 60	16	30	
Gender	Male	25	32	0.5049
	Female	3	8	
Location of tumor	Ce/Ut	4	3	0.4346
	Mt/Lt/Ae	24	37	
Tumor size (mm)	< 50	18	30	0.4206
	⩾ 50	10	10	
Histological type	Differentiated type SCC	25	21	0.0015[a]
	Poorly differentiated type SCC	3	19	
pT	pT1	10	21	0.2191
	pT2-3	18	19	
pN	negative	13	20	0.8095
	positive	15	20	
pStage	Ⅰ	6	16	0.1231
	Ⅱ-Ⅲ	22	24	
Ki-67 labeling index		28.7 ± 2.3	29.9 ± 2.0	0.6834

Ce: Cervical esophagus; Ut: Upper thoracic esophagus; Mt: Middle thoracic esophagus; Lt: Lower thoracic esophagus; Ae: Abdominal esophagus; pT: Pathological T stage; pN: Pathological N stage; pStage: Pathological stage; SCC: Squamous cell carcinoma; [a]$P < 0.05$ *vs* control, Fisher's exact test.

fragmented and hybridized to an Agilent SurePrint G3 Human Gene Expression 8 × 60K Microarray for 17 h. Slides were washed and scanned immediately on an Agilent DNA Microarray Scanner (G2565CA) using the one color scan setting for 8 × 60K array slides.

Processing of microarray data

Scanned images were analyzed with Feature Extraction Software 10.10 (Agilent) using default parameters to obtain background-subtracted and spatially detrended Processed Signal intensities. Signal transduction networks were analyzed with Ingenuity Pathway Analysis (IPA) software (Ingenuity Systems, Inc., Redwood City, CA).

Statistical analysis

Fisher's exact test was used to evaluate the differences between proportions, and Student's *t* tests (for comparisons between two groups) and Tukey-Kramer HSD tests (for multiple comparisons) were used to evaluate continuous variables. Survival curves were constructed by the Kaplan-Meier method, and differences in survival were examined using the log-rank test. Differences were considered significant when the relevant *P* value was < 0.05.

These analyses were performed using the statistical software JMP (version 8, SAS Institute Inc., Cary, NC). Correlation analysis was performed by creating Fit Y by X plots using JMP.

RESULTS

NKCC1 protein expression in human ESCCs

An immunohistochemical examination of non-cancerous esophageal epithelia performed with the NKCC1 antibody demonstrated that cells with NKCC1 expression were chiefly confined to the lower and middle layer of the squamous epithelium but were absent from the basal and parabasal cell layers (Figure 2A). Photographs of well differentiated, moderately differentiated, or poorly differentiated ESCC tumor samples with high or low NKCC1 expression are shown in Figure 2B. NKCC1 expression was observed in the cytoplasm of ESCC cells in all groups. NKCC1 staining scores were significantly increased as histological differentiation decreased (Figure 2C).

We divided ESCC patients into 2 groups, a low grade NKCC1 expression group with staining scores < 6, $n = 28$, and a high grade NKCC1 expression group with staining scores ⩾ 6, $n = 40$, and compared their clinicopathological features. We found that the percentage of poorly differentiated SCC samples was significantly higher in the high grade group (47.5%) when compared to the low grade group (10.7%) (Table 1). No correlation was found between NKCC1 expression and any other clinicopathological parameter. No correlation was found between NKCC1 expression and the Ki-67 labeling index (Table 1). Furthermore, the 5-year survival rate did not differ between the high grade group (69.9 %) and the low grade group (63.5 %) ($P = 0.501$, the log-rank test). Subgroup analysis of pStage I patients showed that the 5-year survival rate of the high grade group (86.5%) tended to be lower than that of the low grade group (100.0 %), although no significant difference was observed ($P = 0.403$, the log-rank test). These results suggest that NKCC1 plays an important role in the differentiation of ESCC cells, although a significant prognostic impact could not be determined.

NKCC1 controls cell cycle progression in ESCC cells

We examined six ESCC cell lines, TE2, TE5, TE9 TE13, KYSE70, and KYSE170, to determine NKCC1 protein expression levels. Western blotting analysis revealed that NKCC1 was highly expressed in the KYSE170 cell line, and lower levels of expression were observed in the TE2 and TE5 cell lines (Figure 3A). We conducted knockdown experiments using NKCC1 siRNA in KYSE170 cells and analyzed the effects of NKCC1 depletion on cell cycle progression. NKCC1 siRNA effectively reduced NKCC1 protein levels (Figure 3B) and NKCC1 mRNA levels (Figure 3C) in the KYSE170 cell line. The downregulation of NKCC1 induced G_2/M phase arrest in KYSE170 cells (Figure 3D). The cell counts of NKCC1 depleted cells were significantly lower when compared to those of control siRNA transfected cells 72 h after siRNA transfection (Figure 3E). Furthermore, the NKCC blocker furosemide significantly inhibited

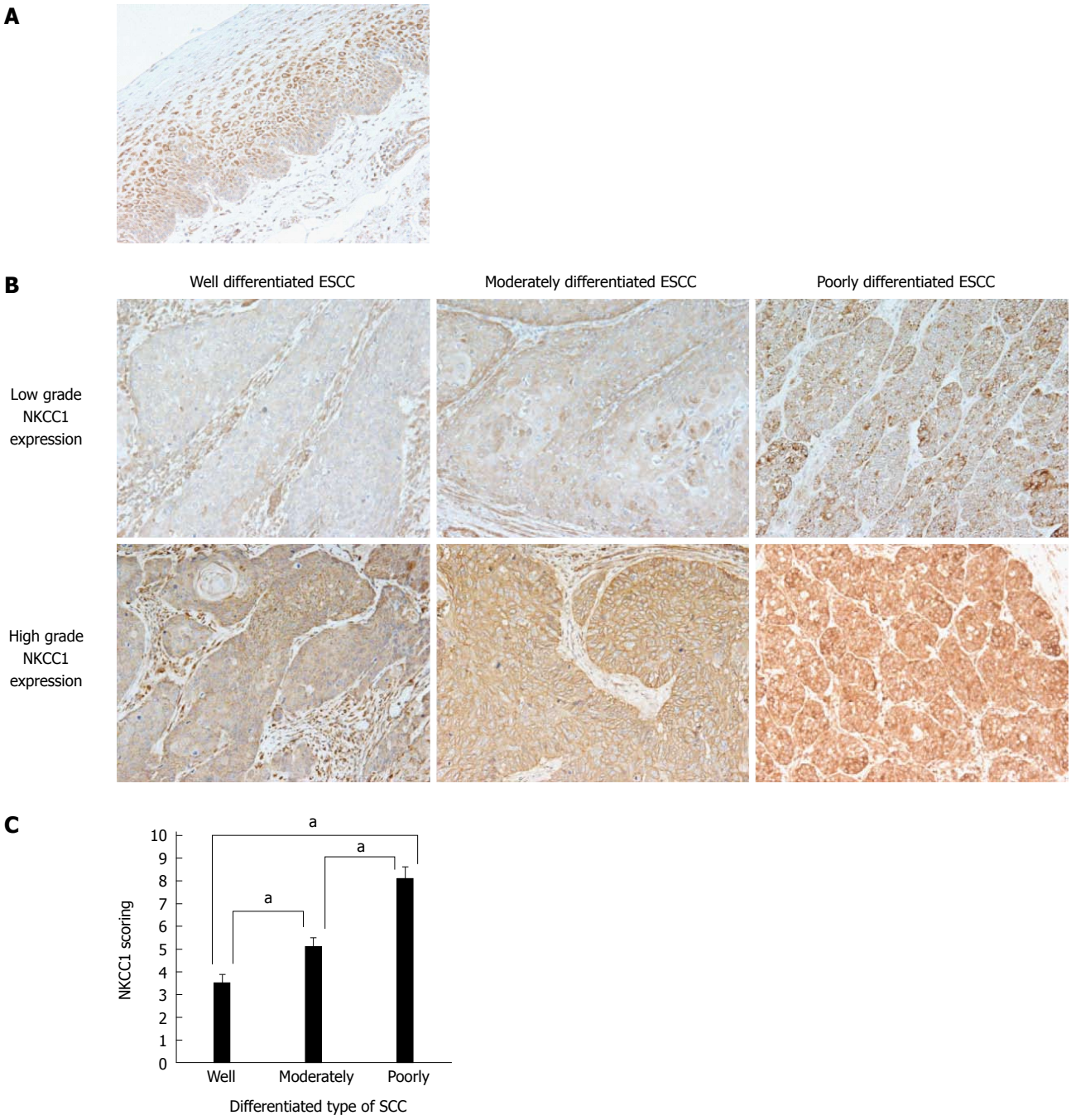

Figure 2 $Na^+/K^+/2Cl^-$ cotransporter 1 protein expression in human esophageal squamous cell carcinomas. A: Immunohistochemical staining of human esophageal epithelia with an $Na^+/K^+/2Cl^-$ cotransporter 1 (NKCC1) antibody. Cells with NKCC1 expression were primarily confined to the lower and middle layers of the squamous epithelium with the exception of the basal and parabasal cell layers; B: Immunohistochemical staining of well differentiated, moderately differentiated, or poorly differentiated esophageal squamous cell carcinoma (ESCC) tumor samples with high or low grade NKCC1 expression (magnification: × 200); C: NKCC1 staining scores according to the differentiation type of SCC. Mean ± SEM. Well differentiated ESCC; n = 15. Moderately differentiated ESCC; n = 31. Poorly differentiated ESCC; n = 22. $^aP < 0.05$ *vs* control, Tukey-Kramer HSD test.

the proliferation of KYSE170 cells (Figure 3F). Similar trends were found in several cell lines, including TE9, TE13 and KYSE 70, which expressed NKCC1 (Figure 4). These results suggest that NKCC1 plays an important role in regulating cell cycle progression and cell proliferation in ESCC cells.

Gene expression profiles of NKCC1 depleted cells

We analyzed the gene expression profiles of NKCC1 depleted KYSE170 cells in microarray and bioinformatics studies. Microarray analysis showed that the expression levels of 2527 genes displayed fold changes of > 2.0 in KYSE170 cells upon depletion of NKCC1. Of these genes, 1157 were upregulated and 1370 were downregulated in NKCC1 siRNA depleted KYSE170 cells. A list of 20 genes with expression levels that were the most strongly up- or downregulated in NKCC1 depleted KYSE170 cells is shown in Table 2. NKCC1 (SLC12A2) expression

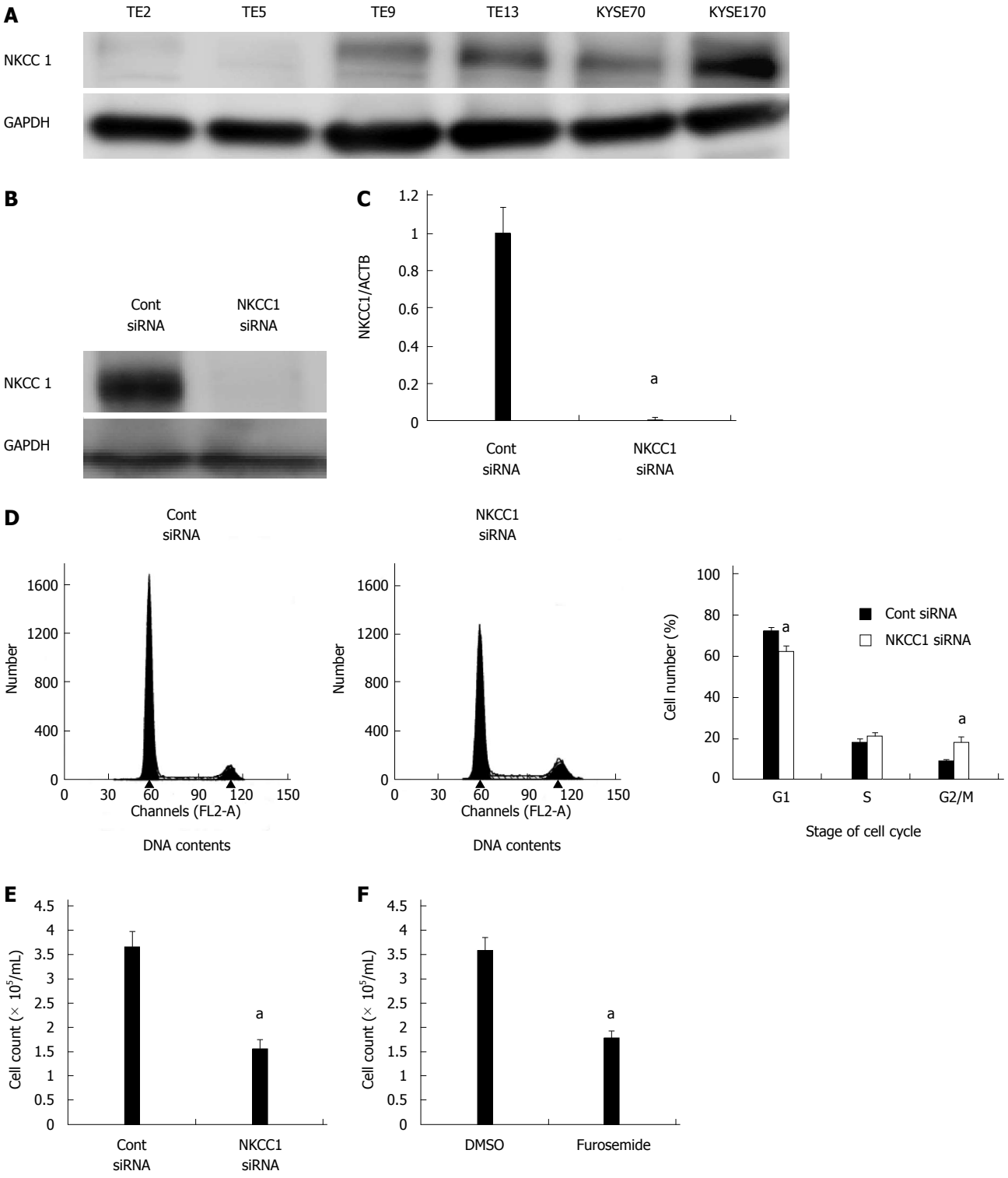

Figure 3 $Na^+/K^+/2Cl^-$ cotransporter 1 controls cell cycle progression in esophageal squamous cell carcinoma cells. A: $Na^+/K^+/2Cl^-$ cotransporter 1 (NKCC1) protein expression was analyzed in 6 esophageal squamous cell carcinoma (ESCC) cell lines. Western blotting revealed that NKCC1 was highly expressed in the KYSE170 cell line, and lower levels of expression were observed in TE2 and TE5 cells. B: Western blotting revealed that NKCC1 small interfering RNA (siRNA) effectively reduced the protein levels of NKCC1 in KYSE170 cells; C: NKCC1 siRNA effectively reduced the mRNA levels of NKCC1 in KYSE170 cells. The mean ± SEM. $n = 4$. $^aP < 0.05$ *vs* the control siRNA group; D: The depletion of NKCC1 induced G_2/M phase arrest in KYSE170 cells. Cells transfected with control or NKCC1 siRNA were stained with propidium iodide (PI) and analyzed by flow cytometry. The mean ± SEM. $n = 5$. $^aP < 0.05$ *vs* control siRNA; E: The depletion of NKCC1 inhibited the proliferation of KYSE170 cells. Cell number was counted 72 h after siRNA transfection. The mean ± SEM. $n = 5$. $^aP < 0.05$ (significantly different from control siRNA); F: The NKCC blocker furosemide inhibited the proliferation of KYSE170 cells. Cell number was counted 72 h after drug stimulation (500 μmol/L furosemide). The mean ± SEM. $n = 5$. $^aP < 0.05$ *vs* control (significantly different from 500 μmol/L DMSO). GAPDH: Glyceraldehyde-3-phosphate dehydrogenase.

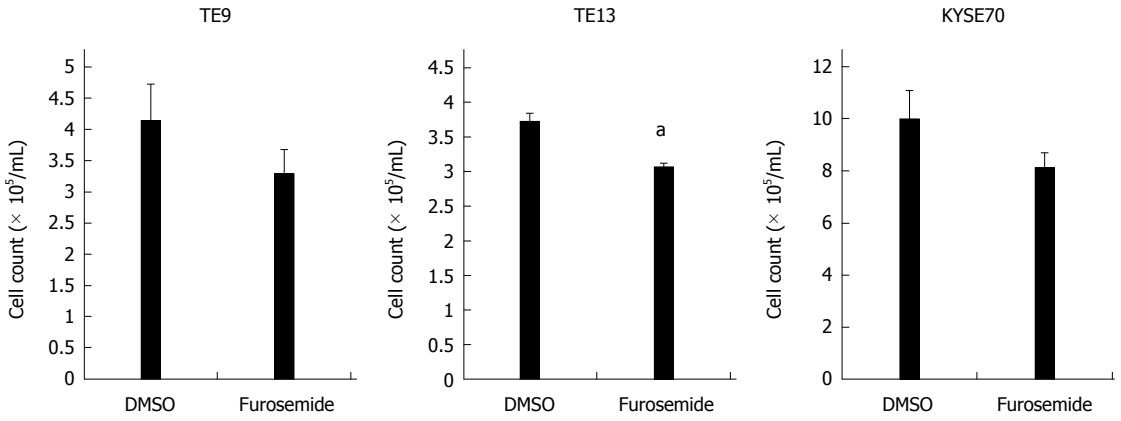

Figure 4 Effects of the $Na^+/K^+/2Cl^-$ cotransporter blocker furosemide on the proliferation of TE9, TE13 and KYSE70 cells. Cell number was counted 72 h after drug stimulation (500 μmol/L furosemide). The mean ± SEM. $n = 3$. $^aP < 0.05$ *vs* control (significantly different from 500 μmol/L DMSO).

Table 2 Twenty genes displaying the highest change in expression levels in $Na^+/K^+/2Cl^-$ cotransporter 1 depleted KYSE170 cells

Gene Symbol	Gene ID	Gene Name	Fold Change
Upregulated Genes			
C18orf34	NM_001105528	Chromosome 18 open reading frame 34	155.49
KCNA6	NM_002235	Potassium voltage-gated channel, shaker-related subfamily, member 6	140.4
CCDC147	NM_001008723	Coiled-coil domain containing 147	105.98
C20orf202	NM_001009612	Chromosome 20 open reading frame 202	86.17
A1CF	NM_138933	APOBEC1 complementation factor	70.98
SH3GL2	NM_003026	SH3-domain GRB2-like 2	70.93
PTGFR	NM_001039585	Prostaglandin F receptor (FP)	66.99
NDN	NM_002487	Necdin homolog (mouse)	66.45
INPP5D	NM_001017915	Inositol polyphosphate-5-phosphatase, 145 kDa	52.83
CYP2E1	NM_000773	Cytochrome P450, family 2, subfamily E, polypeptide 1	52.44
AGBL3	NM_178563	ATP/GTP binding protein-like 3	50.88
UBTFL1	NM_001143975	Upstream binding transcription factor, RNA polymerase Ⅰ-like 1	47.88
PADI2	NM_007365	Peptidyl arginine deiminase, type Ⅱ	46.83
CCR1	NM_001295	Chemokine (C-C motif) receptor 1	44.86
ARC	NM_015193	Activity-regulated cytoskeleton-associated protein	44.41
COLEC10	NM_006438	Homo sapiens collectin sub-family member 10 (C-type lectin)	44.28
DNAH6	NM_001370	Dynein, axonemal, heavy chain 6	41.96
BOLL	NM_033030	Bol, boule-like (Drosophila)	41.31
CORO2B	NM_006091	Coronin, actin binding protein, 2B	41.04
MUC7	NM_152291	Mucin 7, secreted	36.97
Downregulated Genes			
NPFFR1	NM_022146	Neuropeptide FF receptor 1	-54.97
LRRFIP1	NM_001137550	Leucine rich repeat (in FLII) interacting protein 1	-44.72
PPIL6	NM_173672	Peptidylprolyl isomerase (cyclophilin)-like 6	-44.46
CRHR2	NM_001883	Corticotropin releasing hormone receptor 2	-39.78
CMTM2	NM_144673	CKLF-like MARVEL transmembrane domain containing 2	-39.62
C5	NM_001735	Complement component 5	-39.13
KCNMA1	NM_001014797	Potassium large conductance calcium-activated channel, subfamily M, alpha member 1	-38.59
HESX1	NM_003865	HESX homeobox 1	-33.03
SLC22A2	NM_003058	Solute carrier family 22 (organic cation transporter), member 2	-32.49
WNT8B	NM_003393	Wingless-type MMTV integration site family, member 8B	-32.17
GRIA1	NM_000827	Glutamate receptor, ionotropic, AMPA 1	-31.27
ZNF367	NM_153695	Zinc finger protein 367	-30.04
GPR128	NM_032787	G protein-coupled receptor 128	-29.88
SLC12A2	NM_001046	Solute carrier family 12 (sodium/potassium/chloride transporters), member 2	-28.92
KCNG2	NM_012283	Potassium voltage-gated channel, subfamily G, member 2	-28.3
ECT2L	NM_001077706	Epithelial cell transforming sequence 2 oncogene-like	-27
ERMN	NM_020711	Ermin, ERM-like protein	-26.61
DPP10	NM_020868	Dipeptidyl-peptidase 10 (non-functional)	-26.58
TSPAN7	NM_004615	Tetraspanin 7	-25.54
APOA1	NM_000039	Apolipoprotein A-I	-25.21

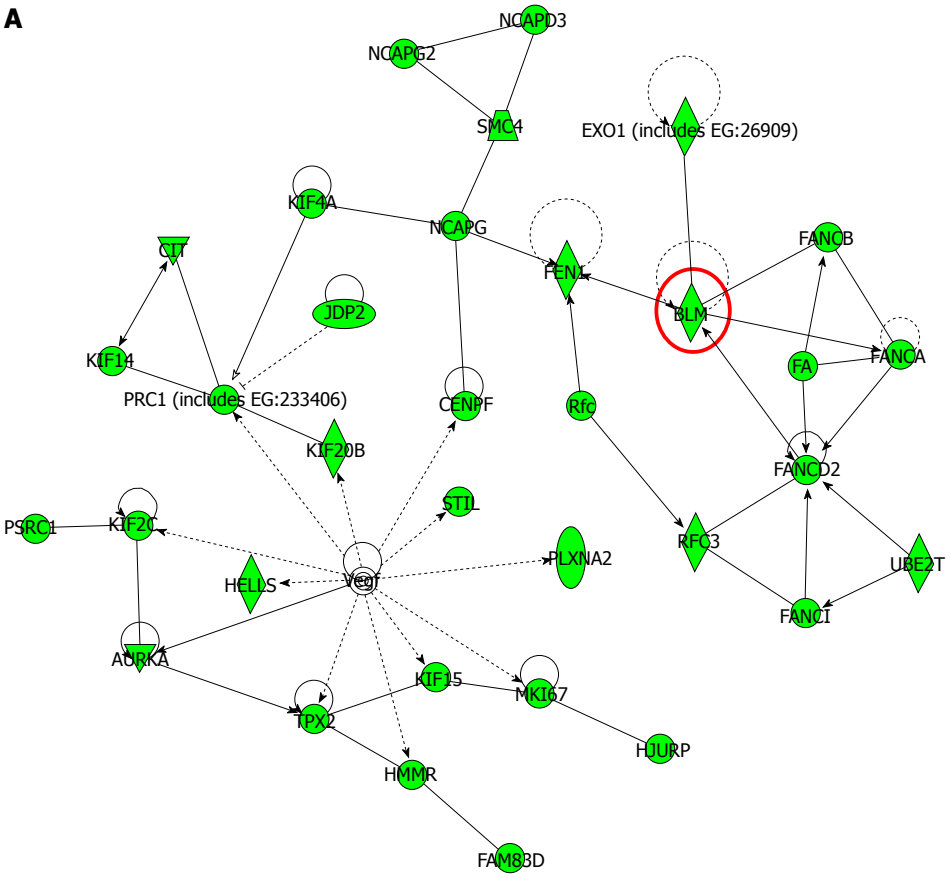
A
NCAPD3
NCAPG2
SMC4
EXO1 (includes EG:26909)
KIF4A
NCAPG
FANCB
CIT
PEN1
JDP2
BLM
KIF14
FA
FANCA
PRC1 (includes EG:233406)
CENPF
Rfc
KIF20B
FANCD2
STIL
PSRC1
KIF2C
RFC3
PLXNA2
UBE2T
HELLS
Ycdf
FANCI
AURKA
KIF15
MKI67
TPX2
HJURP
HMMR
FAM83D

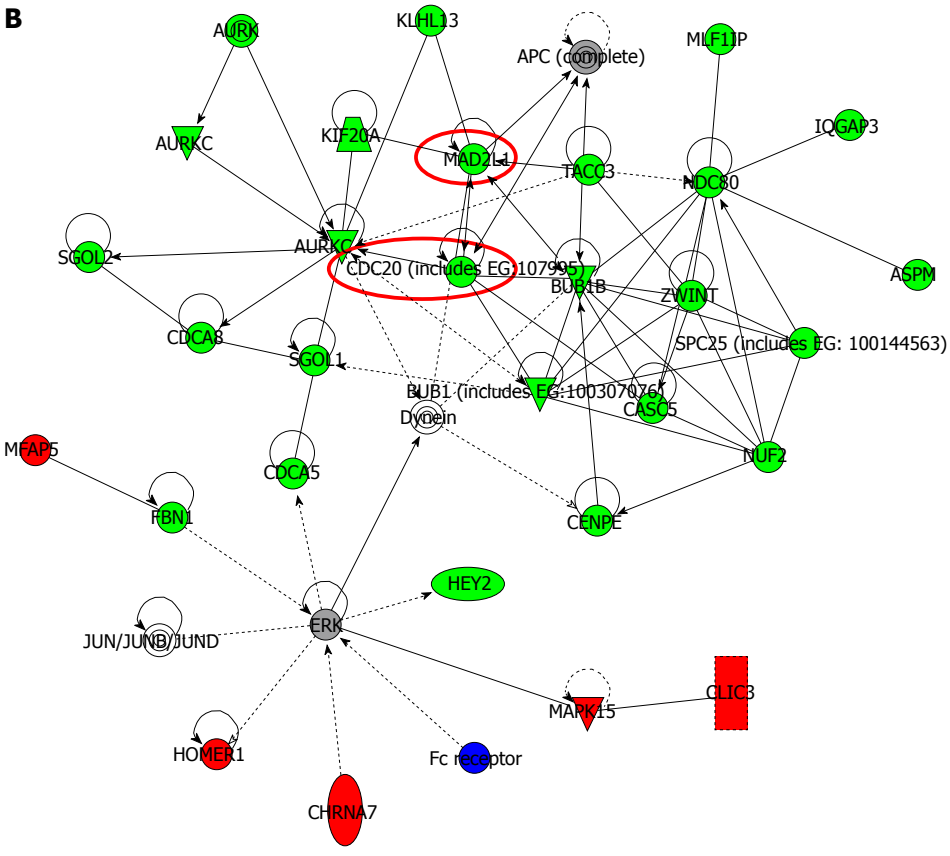
B
AURK
KLHL13
APC (complete)
MLF1IP
AURKC
KIF20A
IQGAP3
MAD2L1
TACC3
NDC80
SGOL2
AURKC
CDC20 (includes EG:107995)
ASPM
BUB1B
ZWINT
CDCA8
SPC25 (includes EG: 100144563)
SGOL1
BUB1 (includes EG:100307076)
Dynein
CASC5
MFAP5
NUF2
CDCA5
FBN1
CENPE
HEY2
ERK
JUN/JUNB/JUND
CLIC3
MAPK15
HOMER1
Fc receptor
CHRNA7

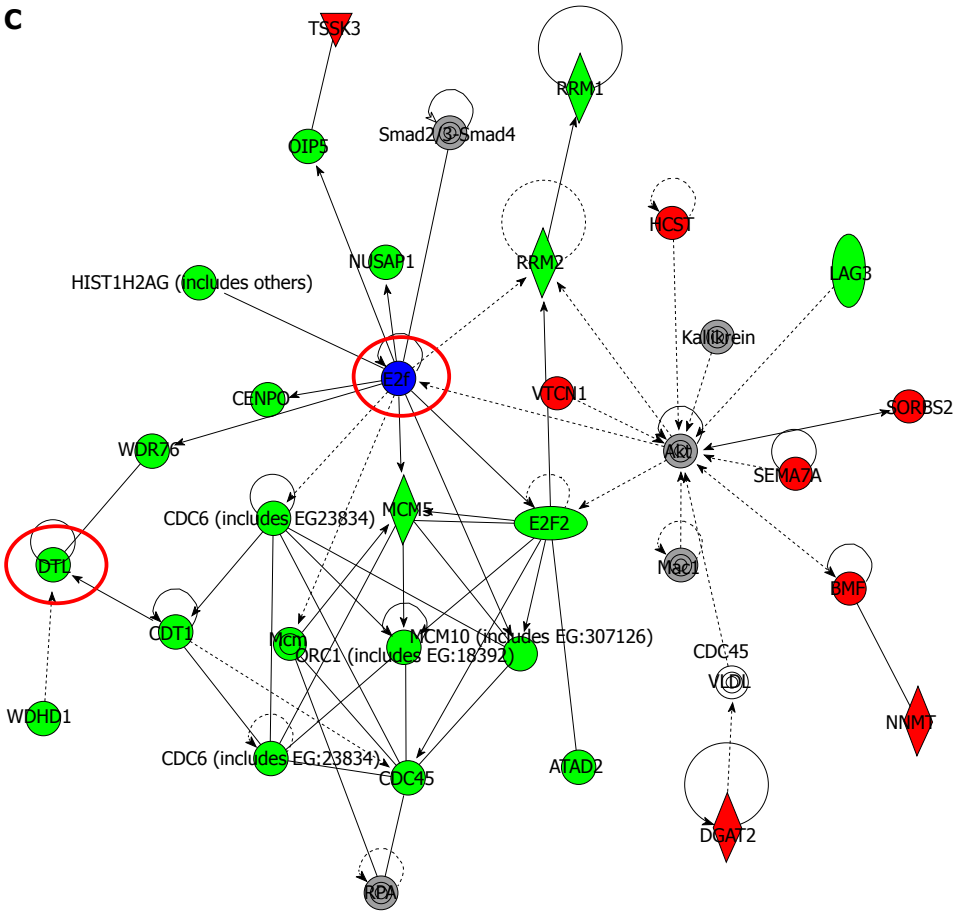

Figure 5 Top-ranked signaling networks related to $Na^+/K^+/2Cl^-$ cotransporter 1 downregulation according to ingenuity pathway analysis. A: This network is called "Cellular Assembly and Organization; DNA Replication, Recombination, and Repair; Cell Cycle"; B: This network is called "Cellular Assembly and Organization, Cell Cycle, DNA Replication, Recombination, and Repair"; C: This network is called "Cell Cycle; DNA Replication, Recombination, and Repair; Cancer". Red and green indicate genes with expression levels that were higher or lower, respectively, than reference RNA levels. Genes analyzed for verification in Figure 6 were highlighted by red circles.

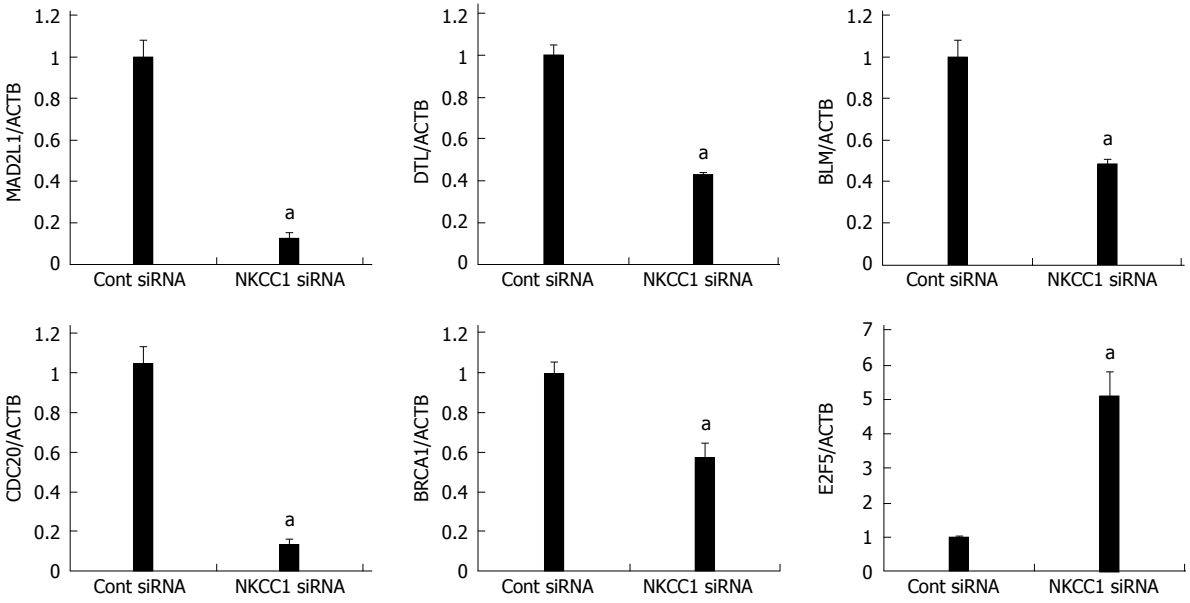

Figure 6 Verification of gene expression by real-time quantitative reverse transcription-polymerase chain reaction. The expression levels of six selected genes (MAD2L1, DTL, BLM, CDC20, BRCA1, and E2F5) in NKCC1 depleted KYSE170 cells were compared to those in control siRNA transfected cells using real-time quantitative reverse transcription-polymerase chain reaction. Gene expression levels were normalized to the level of ACTB. The mean ± SEM. $n = 3$. $^aP < 0.05$ *vs* control siRNA.

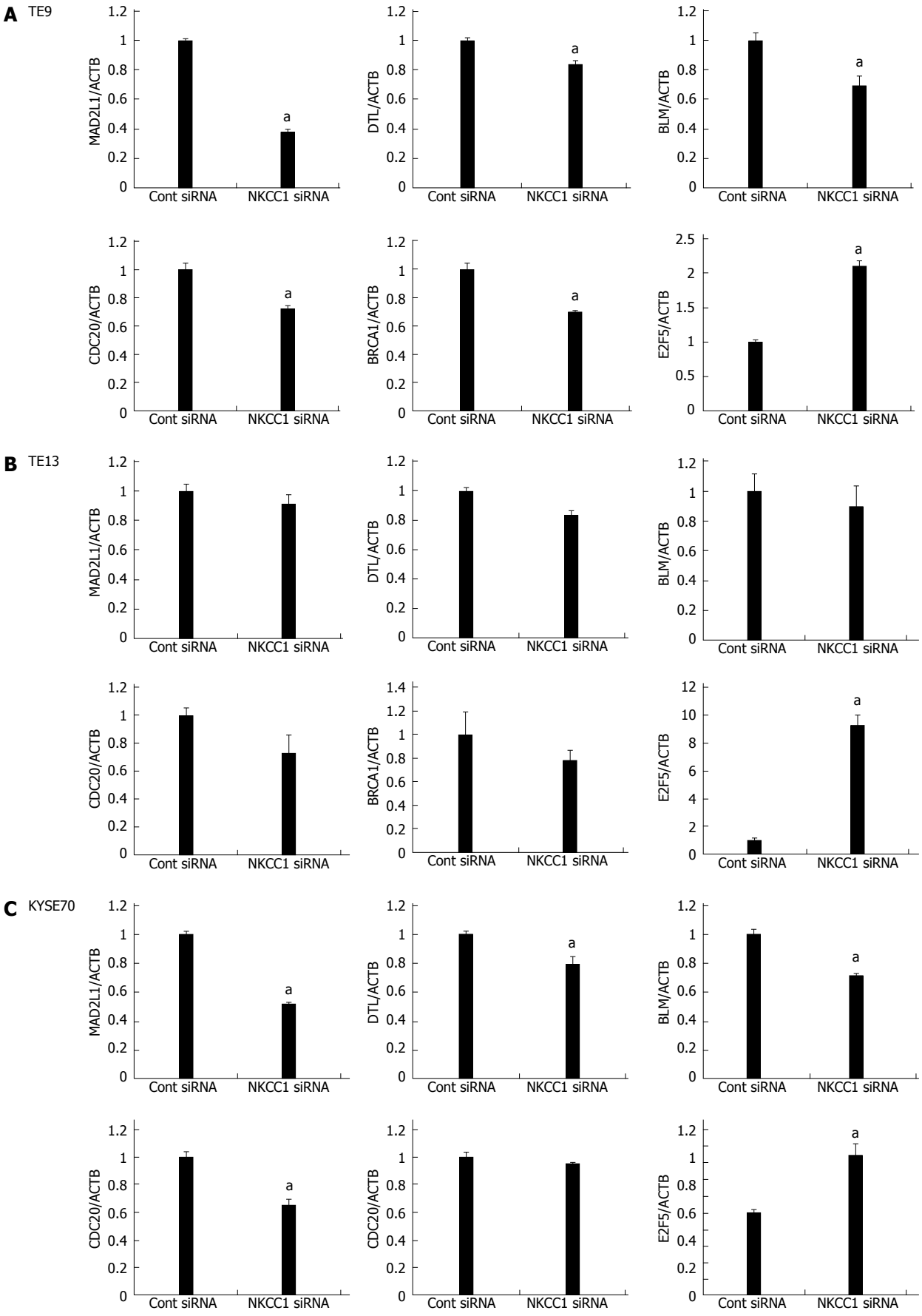

Figure 7 Expression levels of six selected genes (MAD2L1, DTL, BLM, CDC20, BRCA1, and E2F5) in $Na^+/K^+/2Cl^-$ cotransporter 1 depleted TE9, TE13 and KYSE70 cells. The expression levels of six selected genes (MAD2L1, DTL, BLM, CDC20, BRCA1, and E2F5) in $Na^+/K^+/2Cl^-$ cotransporter 1 (NKCC1) depleted TE9 (A), TE13 (B) and KYSE70 cells (C) were compared to those in control siRNA transfected cells using real-time quantitative RT-PCR. Gene expression levels were normalized to the level of ACTB. The mean ± SEM. $n = 3$. $^aP < 0.05$ *vs* control siRNA.

Table 3 Top biological functions, canonical pathways, and networks of $Na^+/K^+/2Cl^-$ cotransporter 1 according to Ingenuity Pathway Analysis

Top Biological Functions		
Diseases and disorders		
Name	*P* value	Number of molecules
Cancer	2.08E-12 - 1.59E-02	277
Gastrointestinal disease	8.03E-12 - 1.60E-02	149
Reproductive system disease	2.25E-09 - 1.57E-02	138
Hematological disease	1.72E-06 - 1.22E-02	70
Hereditary disorder	2.10E-06 - 1.57E-02	120
Molecular and cellular functions		
Name	*P* value	Number of molecules
Cell cycle	1.06E-20 - 1.60E-02	158
Cellular assembly and organization	1.06E-20 - 1.36E-02	111
DNA replication, recombination, and repair	1.06E-20 - 1.16E-02	133
Cellular movement	8.36E-11 - 1.51E-02	82
Cell death	2.98E-06 - 1.56E-02	216
Top canonical pathways		
Name	*P* value	Ratio
Role of BRCA1 in the DNA damage response	9.79E-6	12/65 (0.185)
Mitotic roles of Polo-Like kinase	7.37E-5	11/69 (0.159)
Estrogen-mediated S-phase entry	4.91E-4	6/28 (0.214)
Cell Cycle: G2/M DNA damage checkpoint regulation	5.07E-4	8/49 (0.163)
Role of CHK proteins in cell cycle checkpoint control	5.37E-4	9/56 (0.161)
Top networks		
Associated network functions	Score	
Cellular assembly and organization; DNA replication, recombination, and repair; Cell cycle	47	
Cellular assembly and organization, Cell cycle, DNA replication, recombination, and repair	43	
Cell cycle; DNA replication, recombination, and repair; Cancer	37	
Digestive system development and function, organismal injury and abnormalities, cellular function and maintenance	37	
Cellular assembly and organization; DNA replication, recombination, and repair; Cardiovascular disease	35	

was downregulated in NKCC1 depleted KYSE170 cells (fold change: -28.92; Table 2). Ingenuity Pathway Analysis showed that "Cancer" was the top-ranked disease and that "Cell Cycle" was the top-ranked biological function related to NKCC1 depletion. Furthermore, "Cell Cycle: G2/M DNA Damage Checkpoint Regulation" was one of the top-ranked canonical pathways related to NKCC1 depletion (Table 3), and this result was in agreement with the results obtained *via* cell cycle analysis. Among the 2527 genes with expression levels that were altered by NKCC1 depletion, 267 genes exhibited cell proliferation-related functions (Table 4). Among these genes, 82 genes were upregulated, and the other 185 genes were downregulated. We then examined the signal transduction networks induced by NKCC1 depletion (Table 3). All of the top 3 ranked signal networks were related to the cell cycle (Figure 5). These results indicate that the expression level of NKCC1 influences genes related to cellular growth and cell cycle progression.

Verification of gene expression by real-time quantitative RT-PCR

Six genes (MAD2L1, DTL, BLM, CDC20, BRCA1, and E2F5) were further examined by quantitative Real time reverse transcription-polymerase chain reaction (RT-PCR). BLM was chosen from Network A, MAD2L1 and CDC20 from Network B, and DTL and E2F from Network C (Figure 5). BRCA1 was chosen because "Role of BRCA1 in DNA Damage Response" was the top-ranked canonical pathway related to NKCC1 (Table 3). All of these genes were related to the G2/M checkpoint according to IPA and are included in Table 4. The expression levels of MAD2L1, DTL, BLM, CDC20, and BRCA1 mRNA were significantly lower in NKCC1 depleted KYSE170 cells compared to control siRNA transfected cells (Figure 6). The expression levels of E2F5 mRNA were significantly higher in NKCC1 depleted KYSE170 cells compared to control siRNA transfected cells (Figure 6). Similar trends were found in several cell lines, including TE9, TE13 and KYSE 70 which expressed NKCC1 (Figure 7).These changes were in agreement with the microarray results and suggest that NKCC1 controls cell cycle progression *via* G_2/M checkpoint regulation in ESCC cells.

DISCUSSION

The roles of ion transporters have recently been studied in cancer cells[14,15]. Some types of K^+ channels have been reported to be expressed at high levels in colonic carcinoma[16,17]. The voltage-gated HERG channel has also exhibited cancer-specific expression in gastric can-

Table 4 Cell growth-related genes with expression levels in KYSE170 cells that were changed by the depletion of $Na^+/K^+/2Cl^-$ cotransporter 1

Gene symbol	Gene ID	Biological functions		Fold change
		Cell growth and proliferation	Cell cycle	
Upregulated genes				
NDN	NM_002487	•		66.45
INPP5D	NM_001017915	•	•	52.83
CCR1	NM_001295	•		44.86
COL1A2	NM_000089	•		36.72
EDAR	NM_022336		•	35.86
RBP4	NM_006744	•		30.40
DCLK1	NM_004734		•	28.95
RARRES1	NM_002888	•		22.92
FMOD	NM_002023	•		22.85
BARX1	NM_021570	•		21.47
MAPK10	NM_138980	•		20.00
ADORA2A	NM_000675	•		18.78
CHRNA7	NM_001190455	•	•	18.47
SOX10	NM_006941	•		18.03
FGF20	NM_019851	•		16.73
FAM5C	NM_199051	•	•	14.35
MBD2	NM_015832	•		12.13
EGF	NM_001963	•	•	11.50
TLR5	NM_003268	•		11.35
TNN	NM_022093	•		10.98
SLC1A2	NM_004171	•		10.74
CD36	NM_001001547	•		10.43
CD52	NM_001803	•		10.34
NR2E3	NM_016346	•		10.31
PLCB1	NM_182734		•	10.26
MYCN	NM_005378	•	•	10.23
ZNF365	NM_199451		•	10.12
ERG	NM_004449	•		10.04
MSH4	NM_002440		•	10.03
DMRT1	NM_021951		•	9.61
RNF128	NM_194463	•		9.37
CD69	NM_001781	•		8.89
PDE3A	NM_000921	•	•	8.58
ACVR1C	NM_145259	•		8.57
SPI1	NM_001080547	•	•	8.55
SH2D3C	NM_170600	•		8.53
IFNG	NM_000619	•	•	8.22
MRAS	NM_012219	•		8.20
MCF2L	NM_024979	•		7.43
RRAD	NM_004165	•	•	7.42
E2F5	NM_001951	•	•	7.32
BGN	NM_001711	•		7.13
KIFC1	NM_002263		•	7.02
ABCC6	NM_001171			6.98
SERPINE1	NM_000602	•		6.74
CIITA	NM_000246	•		6.74
GJB6	NM_006783	•		6.45
TP53INP1	NM_033285	•	•	6.38
GHRL	NM_016362	•		6.30
CCNG2	NM_004354	•	•	6.29
RORC	NM_005060	•		6.24
NCF1	NM_000265	•		6.24
NFATC4	NM_001136022	•		6.15
CHRM5	NM_012125	•		6.01
HMOX1	NM_002133	•	•	6.00
IL18RAP	NM_003853	•		5.98
C8orf4	NM_020130	•		5.95
L1CAM	NM_024003	•		5.87
TNFSF8	NM_001244	•		5.85
MSMB	NM_002443	•		5.77
ITPR1	NM_002222	•		5.77
ITGAL	NM_002209	•	•	5.73
INHBA	NM_002192	•	•	5.53
HEYL	NM_014571	•		5.38
JAK3	NM_000215	•	•	5.30
MMP13	NM_002427	•		5.23
NNMT	NM_006169	•		5.06
BNIPL	NM_138278	•		4.86
LTC4S	NM_145867		•	4.74
MMP24	NM_006690	•		4.72
MMP1	NM_002421	•		4.66
CD19	NM_001770	•	•	4.52
ADC	NM_052998	•		4.46
TGFBR1	NM_004612	•	•	4.33
RHOB	NM_004040	•		4.32
CDKN1C	NM_000076	•	•	4.30
HOXB13	NM_006361	•	•	4.20
IPMK	NM_152230	•		4.07
BMF	NM_001003940	•		4.06
VTCN1	NM_024626	•	•	4.05
CEACAM1	NM_001712	•		2.97
TSSK3	NM_052841		•	2.00
Downregulated genes				
CRHR2	NM_001883	•		-39.78
C5	NM_001735	•	•	-39.13
KCNMA1	NM_001014797	•		-38.59
GRIA1	NM_000827	•		-31.27
SLC12A2	NM_001046	•		-28.92
APOA1	NM_000039	•		-25.21
PRKAR2B	NM_002736	•	•	-24.25
TF	NM_001063	•	•	-22.85
BRCA2	NM_000059	•	•	-22.04
AURKC	NM_001015878		•	-21.69
PLXNA4	NM_181775	•		-20.54
TYR	NM_000372	•		-20.39
BACH2	NM_021813	•		-20.01
KIF14	NM_014875		•	-18.06
HEY2	NM_012259	•		-18.01
TMPO	NM_003276	•	•	-15.97
FCGR3A	NM_000569	•		-15.18
ARF6	NM_001663			-15.09
MYBL1	NM_001080416	•	•	-14.60
CCNA1	NM_003914	•	•	-14.29
ESCO2	NM_001017420		•	-14.05
TOP2A	NM_001067	•	•	-13.91
CENPI	NM_006733		•	-13.87
ATAD2	NM_014109	•		-13.41
POSTN	NM_006475	•		-12.91
MKI67	NM_002417	•	•	-12.41
ABCB1	NM_000927	•	•	-12.15
KIF20B	NM_016195	•	•	-11.53
SPN	NM_001030288	•		-11.41
MAD2L1	NM_002358	•	•	-11.16
HLA-DPB1	NM_002121	•		-11.12
SGOL1	NM_001012410		•	-10.91
RRM2	NM_001034	•		-10.71
FANCD2	NM_033084	•	•	-10.55
FANCA	NM_001018112	•	•	-10.31
HDAC2	NM_001527	•	•	-9.94
NUF2	NM_145697		•	-9.76
CLSPN	NM_022111	•	•	-9.57
RAD54L	NM_003579		•	-9.47
KLHL13	NM_033495		•	-9.32
CCNA2	NM_001237	•	•	-9.13
MCM10	NM_182751	•	•	-9.11
MCTS1	NM_014060	•		-9.02
ANLN	NM_018685		•	-9.00
HMGB2	NM_002129	•	•	-8.86
VPREB1	NM_007128	•		-8.81
KIF4A	NM_012310		•	-8.78
SPC25	NM_020675		•	-8.75
ALOX5	NM_000698	•	•	-8.55

PBK	NM_018492	•		-8.20
TNFRSF11B	NM_002546	•		-8.20
CIT	NM_001206999		•	-8.17
HELLS	NM_018063	•	•	-8.1
CDC45	NM_003504	•	•	-8.07
DTL	NM_016448	•	•	-8.00
RGS3	NM_017790			-7.93
TYMS	NM_001071	•	•	-7.87
NDC80	NM_006101		•	-7.86
ERCC6L	NM_017669		•	-7.82
CENPE	NM_001813		•	-7.75
TTK	NM_003318	•	•	-7.74
SIM2	NM_009586		•	-7.61
KRT4	NM_002272	•		-7.55
RAD51AP1	NM_006479		•	-7.55
LTA	NM_000595	•		-7.51
PAK2	NM_002577	•	•	-7.50
SLC5A8	NM_145913	•		-7.41
BLM	NM_000057	•	•	-7.40
NUSAP1	NM_016359		•	-7.36
JDP2	NM_130469	•	•	-7.19
CASP3	NM_004346	•	•	-7.17
NEIL3	NM_018248	•		-7.17
POLH	NM_006502	•	•	-7.11
KIF20A	NM_005733	•	•	-7.08
MYO7A	NM_000260			-6.93
NRGN	NM_006176	•		-6.82
NCAPG	NM_022346	•	•	-6.78
CDCA8	NM_018101	•	•	-6.72
CEP55	NM_018131		•	-6.65
DLGAP5	NM_014750	•	•	-6.60
CDC25C	NM_001790	•	•	-6.59
ARL2BP	NM_012106	•		-6.58
IL12A	NM_000882	•	•	-6.53
MYH14	NM_001077186	•		-6.52
SKA1	NM_001039535		•	-6.46
CASC1	NM_018272		•	-6.44
HJURP	NM_018410		•	-6.42
TACC3	NM_006342	•	•	-6.33
ENPP3	NM_005021	•		-6.30
STIL	NM_001048166	•	•	-6.27
KNTC1	NM_014708		•	-6.26
NR1I2	NM_003889	•	•	-6.24
AKR1B10	NM_020299	•		-6.22
E2F2	NM_004091	•	•	-6.20
USP47	NM_017944	•		-6.14
KIF11	NM_004523	•	•	-6.09
E2F8	NM_024680	•	•	-6.05
PLK1	NM_005030	•	•	-6.02
CCDC6	NM_005436	•		-6.00
ORC6	NM_014321		•	-6.00
EXO1	NM_003686		•	-5.95
GPC5	NM_004466	•		-5.94
GSG2	NM_031965		•	-5.93
PRC1	NM_003981		•	-5.89
RAD51	NM_002875	•	•	-5.78
KIF2C	NM_006845	•	•	-5.71
TNFRSF13C	NM_052945	•		-5.70
BLZF1	NM_003666	•		-5.63
FEN1	NM_004111	•		-5.51
PLK4	NM_014264	•	•	-5.49
HAS2	NM_005328	•	•	-5.44
PKMYT1	NM_182687		•	-5.40
BUB1	NM_001211	•	•	-5.34
BUB1B	NM_001211	•	•	-5.34
NEK2	NM_002497	•	•	-5.33
IQGAP3	NM_178229		•	-5.27
SKA3	NM_145061		•	-5.23
PNN	NM_002687	•	•	-5.20
NTRK3	NM_001007156	•	•	-5.17
IL25	NM_022789	•		-5.09
UBE2C	NM_181803	•	•	-5.09
AURKB	NM_004217	•	•	-5.08
CDC6	NM_001254	•	•	-5.08
CDKN2C	NM_078626	•	•	-5.06
EDN2	NM_001956	•		-5.06
CDC20	NM_001255	•	•	-5.05
RRM1	NM_001033	•	•	-5.05
APC	NM_000038	•	•	-5.04
KIF15	NM_020242	•	•	-5.03
LMNB1	NM_005573	•		-5.02
NCAPG2	NM_017760		•	-4.96
CCNE2	NM_057749	•	•	-4.94
HMMR	NM_012484	•		-4.93
BRIP1	NM_032043	•		-4.90
ECT2	NM_018098	•	•	-4.89
CDT1	NM_030928	•	•	-4.87
MCAM	NM_006500	•		-4.82
LAG3	NM_002286	•	•	-4.78
ZWINT	NM_032997		•	-4.73
DCLK2	NM_001040260		•	-4.72
TRAIP	NM_005879	•		-4.71
SSTR2	NM_001050	•	•	-4.69
TXK	NM_003328	•		-4.65
TBC1D9	NM_015130	•		-4.63
IL1RN	NM_173843	•		-4.61
CDCA7	NM_031942	•		-4.56
STK38	NM_007271	•	•	-4.56
CDCA5	NM_080668	•	•	-4.54
E2F7	NM_203394	•		-4.54
FIGNL1	NM_001042762	•		-4.51
SMC4	NM_005496		•	-4.50
CYCS	NM_018947	•		-4.48
FBN1	NM_000138	•		-4.48
NCAPD3	NM_015261		•	-4.46
IL16	NM_172217	•	•	-4.44
PCNA	NM_002592	•	•	-4.42
FBXO5	NM_001142522		•	-4.37
CKAP2	NM_018204		•	-4.34
IL34	NM_152456	•		-4.34
PSRC1	NM_032636	•	•	-4.33
C11orf82	NM_145018		•	-4.32
CHRDL1	NM_145234		•	-4.31
RAD54B	NM_012415		•	-4.31
DIAPH3	NM_001042517		•	-4.29
AKR1C1	NM_001353	•		-4.26
INHBB	NM_002193	•		-4.25
MDM2	NM_002392	•	•	-4.25
PRKAA1	NM_206907	•		-4.25
MASTL	NM_032844		•	-4.23
MCM5	NM_006739	•		-4.21
CD2AP	NM_012120	•	•	-4.20
BRCA1	NM_007300	•	•	-4.18
TPX2	NM_012112	•	•	-4.15
FGFBP1	NM_005130	•		-4.14
EIF4G2	NM_001172705	•	•	-4.12
AURKA	NM_198433	•	•	-4.10
PTTG1	NM_004219	•	•	-4.08
ADRA1B	NM_000679	•	•	-4.07
RECQL4	NM_004260	•		-4.02
GJB2	NM_004004	•		-4.00
BIRC5	NM_001012271	•	•	-3.35
TERF1	NM_017489	•	•	-3.18
LRP1	NM_032832	•		-2.43
CDK1	NM_012395	•	•	-2.21
ARHGEF10	NM_014629		•	-2.08

cer and its blocker diminished the G_1 to S phase transition[18]. Increased mRNA levels of Ca^{2+} channels have also been reported in colorectal adenocarcinoma[19,20]. Furthermore, some reports have indicated that Cl^- channels/transporters, such as Cl^- channels, K^+/Cl^- cotransporters, and NKCC play important roles in the proliferation of colorectal, breast, lung, and prostate cancer cells[14,15]. To the best of our knowledge, the present study is the first report examining NKCC1 expression in ESCC tissue and the gene expression profile of NKCC1 depleted cancer cells.

We investigated the role of transepithelial Cl^- transport in cancer cells[5-7]. In the present study, we found that the depletion of NKCC1 induced G_2/M phase arrest in KYSE170 cells. We have previously shown that the blockage of NKCC inhibited G_1/S cell cycle progression in gastric and prostate cancer cells[8,9], which suggests that the mechanism by which NKCC1 regulates cell cycle progression varies among cell types and their different genetic backgrounds. Microarray analysis showed that many of the genes that displayed changes in expression levels after NKCC1 depletion were well connected in the top-ranked signaling network related to the cell cycle, indicating that they are not only functionally related but are also regulated together at the level of expression by NKCC1-related signal transduction pathways.

With regard to signaling networks, we noted that the expression levels of several G_2/M checkpoint-related genes were altered by the depletion of NKCC1. In the spindle checkpoint, the anaphase-promoting complex (APC) was activated by CDC20, which subsequently triggered anaphase. MAD2L1, a mitotic spindle assembly checkpoint protein, inhibited the activity of the APC by a direct physical interaction with a ternary complex containing CDC20[21,22]. DTL, BLM, BRCA1, and E2F5 are also known regulators of the G_2/M checkpoint[23-26]. One possible mechanism by which NKCC1 changes the expression of these major G_2/M checkpoint-related genes may be through the regulation of intracellular Cl^- concentrations ($[Cl]_i$). Recent reports have indicated that $[Cl]_i$ is a fundamental signal mediator for the regulation of various cellular functions[27-29]. For example, our study showed that $[Cl]_i$ could act as a signal to regulate mRNA expression of the epithelial Na^+ channel *via* a protein tyrosine kinase-dependent pathway in renal epithelial cells[29]. We have also previously shown that $[Cl]_i$ regulated cell proliferation in gastric and prostate cancer cells[5-9]. We consider NKCC to be one of the important transporters that regulates $[Cl]_i$ in the steady state and have previously shown that the blockage of NKCC decreased $[Cl]_i$[9]. Although the detailed mechanism should be verified by further studies, these observations suggest that the change in $[Cl]_i$ induced by NKCC1 may be a critically important messenger that regulates the expression of these G_2/M checkpoint-related genes in ESCC cells.

Our results demonstrate that no correlation was found between NKCC1 expression and the Ki-67 labeling index in immunohistochemical studies of ESCC expression. Ki-67 is commonly used to assess cell proliferation, and this factor reacts with a nuclear antigen present throughout the cell cycle (late G_1, S, G_2, and M phase) of proliferating cells but is absent from quiescent (G_0) cells[30]. In the present study, we found that NKCC1 plays an important role in the G_2/M phase of the cell cycle. The different rates of progression through each phase of the cell cycle may explain why no correlation was found between NKCC1 and Ki-67 expression, although further studies will be needed with a larger sample size to confirm these observations. Furthermore, in the present study NKCC1 expression was correlated with the degree of histological differentiation in SCC. Similarly, we previously found that mRNA levels and the functional expression levels of NKCC1 were higher in poorly differentiated type gastric adenocarcinoma cells compared to differentiated cells[8]. Furosemide (a NKCC blocker and a loop diuretic) is often used as a diuretic to maintain urine output and improve edema, ascites, or pleural effusion for the treatment of patients with terminal stage cancers. From this viewpoint, our observation that the blockage of NKCC1 diminished the proliferation of ESCC cells provides strong clinical evidence that furosemide can be used for ESCC patients with high NKCC1 expression, such as those with poorly differentiated SCC, and suggests the possibility of a novel tailor-made treatment.

In summary, we found that NKCC1 plays a role in the proliferation of ESCC cells. An immunohistochemical analysis revealed that the expression of NKCC1 in human ESCC samples was related to the histological type of ESCC. Our microarray results also suggest that NKCC1 exhibits marked effects on the expression of genes related to G_2/M cell cycle progression. A deeper understanding of the role of NKCC1 may lead to its use as an important biomarker of tumor development and/or a novel therapeutic target for ESCC.

COMMENTS

Background

The roles of ion transporters have recently been studied in cancer cells, and several reports have demonstrated the important roles of Cl^- channels/transporters in gastrointestinal cancer cells.

Research frontiers

Although previous reports showed that the $Na^+/K^+/2Cl^-$ cotransporter 1 (NKCC1) plays an important role in the proliferation of several types of cancer cells, its role in esophageal squamous cell carcinoma (ESCC) cells has not been fully investigated. Furthermore, the clinicopathological meaning of NKCC1 expression in ESCCs remains uncertain.

Innovations and breakthroughs

The authors analyzed the expression of NKCC1 in human ESCC samples and determined its relationship with the degree of histological differentiation of SCC samples. Depletion of NKCC1 in KYSE170 cells inhibited cell proliferation *via* G_2/M phase arrest. The results of microarray showed that the top-ranked canonical pathway was the G_2/M DNA damage checkpoint regulation pathway, which involves MAD2L1, DTL, BLM, CDC20, BRCA1, and E2F5.

Applications

The study results suggest that a deeper understanding of the role of NKCC1 may lead to its use as an important biomarker of tumor development and/or a novel therapeutic target for ESCC. The observation that the blockage of

NKCC1 diminished the proliferation of ESCC cells provides clinical evidence that furosemide can be used for ESCC patients with high NKCC1 expression, and suggests the possibility of a novel tailor-made treatment.

Terminology

NKCC is a member of the cation-chloride cotransporter family. NKCC transports one sodium ion, one potassium ion, and two chloride ions across the plasma membrane and is sensitive to loop diuretics. There are two isoforms of NKCC, and NKCC1 is ubiquitously expressed in various types of cells including epithelial cells.

Peer review

This is a good descriptive study in which the authors analyzed the role of NKCC1 in the proliferation of ESCC. The authors showed NKCC1 was found in the cytoplasm and related to tumor differentiation in patients with ESCC. Depletion of NKCC1 lead to inhibition of cell proliferation, and microarray analysis showed that NKCC1 exhibits marked effects on the expression of genes related to G_2/M cell cycle progression. The results are interesting and meaningful for further understand the role of NKCC1 on cancer development.

REFERENCES

1 **Bustin SA**, Li SR, Dorudi S. Expression of the Ca2+-activated chloride channel genes CLCA1 and CLCA2 is downregulated in human colorectal cancer. *DNA Cell Biol* 2001; **20**: 331-338 [PMID: 11445004 DOI: 10.1089/104454901521224 42]

2 **Sarosi GA**, Jaiswal K, Herndon E, Lopez-Guzman C, Spechler SJ, Souza RF. Acid increases MAPK-mediated proliferation in Barrett's esophageal adenocarcinoma cells via intracellular acidification through a Cl-/HCO3- exchanger. *Am J Physiol Gastrointest Liver Physiol* 2005; **289**: G991-G997 [PMID: 16081761 DOI: 10.1152/ajpgi.00215.2005]

3 **Hebert SC**, Mount DB, Gamba G. Molecular physiology of cation-coupled Cl- cotransport: the SLC12 family. *Pflugers Arch* 2004; **447**: 580-593 [PMID: 12739168 DOI: 10.1007/s00424-003-1066-3]

4 **Mount DB**, Mercado A, Song L, Xu J, George AL, Delpire E, Gamba G. Cloning and characterization of KCC3 and KCC4, new members of the cation-chloride cotransporter gene family. *J Biol Chem* 1999; **274**: 16355-16362 [PMID: 10347194 DOI: 10.1152/physrev.00011.2004]

5 **Shiozaki A**, Otsuji E, Marunaka Y. Intracellular chloride regulates the G(1)/S cell cycle progression in gastric cancer cells. *World J Gastrointest Oncol* 2011; **3**: 119-122 [PMID: 22007274 DOI: 10.4251/wjgo.v3.i8.119]

6 **Miyazaki H**, Shiozaki A, Niisato N, Ohsawa R, Itoi H, Ueda Y, Otsuji E, Yamagishi H, Iwasaki Y, Nakano T, Nakahari T, Marunaka Y. Chloride ions control the G1/S cell-cycle checkpoint by regulating the expression of p21 through a p53-independent pathway in human gastric cancer cells. *Biochem Biophys Res Commun* 2008; **366**: 506-512 [PMID: 18067855 DOI: 10.1016/j.bbrc.2007.11.144]

7 **Ohsawa R**, Miyazaki H, Niisato N, Shiozaki A, Iwasaki Y, Otsuji E, Marunaka Y. Intracellular chloride regulates cell proliferation through the activation of stress-activated protein kinases in MKN28 human gastric cancer cells. *J Cell Physiol* 2010; **223**: 764-770 [PMID: 20205250 DOI: 10.1002/jcp.22088]

8 **Shiozaki A**, Miyazaki H, Niisato N, Nakahari T, Iwasaki Y, Itoi H, Ueda Y, Yamagishi H, Marunaka Y. Furosemide, a blocker of Na+/K+/2Cl- cotransporter, diminishes proliferation of poorly differentiated human gastric cancer cells by affecting G0/G1 state. *J Physiol Sci* 2006; **56**: 401-406 [PMID: 17052386 DOI: 10.2170/physiolsci.RP010806]

9 **Hiraoka K**, Miyazaki H, Niisato N, Iwasaki Y, Kawauchi A, Miki T, Marunaka Y. Chloride ion modulates cell proliferation of human androgen-independent prostatic cancer cell. *Cell Physiol Biochem* 2010; **25**: 379-388 [PMID: 20332618 DOI: 10.1159/000303042]

10 **Nishihira T**, Hashimoto Y, Katayama M, Mori S, Kuroki T. Molecular and cellular features of esophageal cancer cells. *J Cancer Res Clin Oncol* 1993; **119**: 441-449 [PMID: 8509434]

11 **Shimada Y**, Imamura M, Wagata T, Yamaguchi N, Tobe T. Characterization of 21 newly established esophageal cancer cell lines. *Cancer* 1992; **69**: 277-284 [PMID: 1728357]

12 **Sobin L**, Gospodarowicz M, Wittekind C, eds. TNM Classification of malignant tumors. 7th ed. Hoboken, NJ: John Wiley Sons, Inc, 2009

13 **Remmele W**, Stegner HE. [Recommendation for uniform definition of an immunoreactive score (IRS) for immunohistochemical estrogen receptor detection (ER-ICA) in breast cancer tissue]. *Pathologe* 1987; **8**: 138-140 [PMID: 3303008]

14 **Kunzelmann K**. Ion channels and cancer. *J Membr Biol* 2005; **205**: 159-173 [PMID: 16362504 DOI: 10.1007/s00232-005-0781-4]

15 **Schönherr R**. Clinical relevance of ion channels for diagnosis and therapy of cancer. *J Membr Biol* 2005; **205**: 175-184 [PMID: 16362505 DOI: 10.1007/s00232-005-0782-3]

16 **Lastraioli E**, Guasti L, Crociani O, Polvani S, Hofmann G, Witchel H, Bencini L, Calistri M, Messerini L, Scatizzi M, Moretti R, Wanke E, Olivotto M, Mugnai G, Arcangeli A. herg1 gene and HERG1 protein are overexpressed in colorectal cancers and regulate cell invasion of tumor cells. *Cancer Res* 2004; **64**: 606-611 [PMID: 14744775 DOI: 10.1158/0008-5472.CAN-03-2360]

17 **Kim CJ**, Cho YG, Jeong SW, Kim YS, Kim SY, Nam SW, Lee SH, Yoo NJ, Lee JY, Park WS. Altered expression of KCNK9 in colorectal cancers. *APMIS* 2004; **112**: 588-594 [PMID: 15601307 DOI: 10.1111/j.1600-0463.2004.apm1120905.x]

18 **Shao XD**, Wu KC, Hao ZM, Hong L, Zhang J, Fan DM. The potent inhibitory effects of cisapride, a specific blocker for human ether-a-go-go-related gene (HERG) channel, on gastric cancer cells. *Cancer Biol Ther* 2005; **4**: 295-301 [PMID: 15846098 DOI: 10.4161/cbt.4.3.1500]

19 **Wang XT**, Nagaba Y, Cross HS, Wrba F, Zhang L, Guggino SE. The mRNA of L-type calcium channel elevated in colon cancer: protein distribution in normal and cancerous colon. *Am J Pathol* 2000; **157**: 1549-1562 [PMID: 11073814 DOI: 10.1016/S0002-9440(10)64792-X]

20 **Tsavaler L**, Shapero MH, Morkowski S, Laus R. Trp-p8, a novel prostate-specific gene, is up-regulated in prostate cancer and other malignancies and shares high homology with transient receptor potential calcium channel proteins. *Cancer Res* 2001; **61**: 3760-3769 [PMID: 11325849]

21 **Luo X**, Fang G, Coldiron M, Lin Y, Yu H, Kirschner MW, Wagner G. Structure of the Mad2 spindle assembly checkpoint protein and its interaction with Cdc20. *Nat Struct Biol* 2000; **7**: 224-229 [PMID: 10700282 DOI: 10.1038/73338]

22 **Luo X**, Tang Z, Xia G, Wassmann K, Matsumoto T, Rizo J, Yu H. The Mad2 spindle checkpoint protein has two distinct natively folded states. *Nat Struct Mol Biol* 2004; **11**: 338-345 [PMID: 15024386 DOI: 10.1016/S1097-2765(01)00435-X]

23 **Sansam CL**, Shepard JL, Lai K, Ianari A, Danielian PS, Amsterdam A, Hopkins N, Lees JA. DTL/CDT2 is essential for both CDT1 regulation and the early G2/M checkpoint. *Genes Dev* 2006; **20**: 3117-3129 [PMID: 17085480 DOI: 10.1101/gad.1482106]

24 **Ababou M**, Dutertre S, Lécluse Y, Onclercq R, Chatton B, Amor-Guéret M. ATM-dependent phosphorylation and accumulation of endogenous BLM protein in response to ionizing radiation. *Oncogene* 2000; **19**: 5955-5963 [PMID: 11146546]

25 **Shabbeer S**, Omer D, Berneman D, Weitzman O, Alpaugh A, Pietraszkiewicz A, Metsuyanim S, Shainskaya A, Papa MZ, Yarden RI. BRCA1 targets G2/M cell cycle proteins for ubiquitination and proteasomal degradation. *Oncogene* 2013; **32**: 5005-5016 [PMID: 23246971 DOI: 10.1038/onc.2012.522]

26 **Wan Z**, Zhi N, Wong S, Keyvanfar K, Liu D, Raghavachari N, Munson PJ, Su S, Malide D, Kajigaya S, Young NS. Human parvovirus B19 causes cell cycle arrest of human erythroid progenitors via deregulation of the E2F family of transcription factors. *J Clin Invest* 2010; **120**: 3530-3544 [PMID:

20890043 DOI: 10.1172/JCI41805]
27 **Jiang B**, Hattori N, Liu B, Nakayama Y, Kitagawa K, Sumita K, Inagaki C. Expression and roles of Cl- channel ClC-5 in cell cycles of myeloid cells. *Biochem Biophys Res Commun* 2004; **317**: 192-197 [PMID: 15047167 DOI: 10.1016/j.bbrc.2004.03.036]
28 **Menegazzi R**, Busetto S, Dri P, Cramer R, Patriarca P. Chloride ion efflux regulates adherence, spreading, and respiratory burst of neutrophils stimulated by tumor necrosis factor-alpha (TNF) on biologic surfaces. *J Cell Biol* 1996; **135**: 511-522 [PMID: 8896606]
29 **Niisato N**, Eaton DC, Marunaka Y. Involvement of cytosolic Cl- in osmoregulation of alpha-ENaC gene expression. *Am J Physiol Renal Physiol* 2004; **287**: F932-F939 [PMID: 15292045 DOI: 10.1152/ajprenal.00131.2004]
30 **Gerdes J**, Lemke H, Baisch H, Wacker HH, Schwab U, Stein H. Cell cycle analysis of a cell proliferation-associated human nuclear antigen defined by the monoclonal antibody Ki-67. *J Immunol* 1984; **133**: 1710-1715 [PMID: 6206131]

P- Reviewers: Kim MP, Zhao BS
S- Editor: Qi Y **L- Editor**: A **E- Editor**: Liu XM

Published by **Baishideng Publishing Group Inc**
8226 Regency Drive, Pleasanton, CA 94588, USA
Telephone: +1-925-223-8242
Fax: +1-925-223-8243
E-mail: bpgoffice@wjgnet.com
Help Desk: http://www.wjgnet.com/esps/helpdesk.aspx
http://www.wjgnet.com

ISSN 1007-9327

© 2014 Baishideng Publishing Group Inc. All rights reserved.